Quantifying sensitivity of aerosol-cloud interactions to atmospheric state through cluster analysis

W.S.J. Kroese
5434947

ADDITIONAL MASTER THESIS

submitted in partial fulfillment of the
requirements for the degree of

MASTER OF SCIENCE
in
APPLIED EARTH SCIENCES

SRON Supervisors:	Dr. Bastiaan van Diedenhoven
	Dr. Otto Hasekamp
TU Delft Supervisors:	Dr.sc. Franziska Glassmeier
	Dr. Marc Schleiss

Delft, The Netherlands, December 24, 2022

Quantifying sensitivity of aerosol-cloud interactions to atmospheric state through cluster analysis

W.S.J. Kroese

Civil Engineering and Earth Sciences, TU Delft
Stevinweg 1, 2628 CN, Delft, The Netherlands

December 24, 2022

Abstract

Cloud droplet number concentrations change due to perturbations in aerosol concentrations. The strength of this correlation covaries with meteorology. Using polarimetric aerosol estimates and MODIS-2 cloud retrievals we compute the interaction strength per meteorological regime, which we determined using clustering techniques on MERRA-2 reanalysis data. The clusters that were found are similar to other clustering studies. The clusters are however not well-separated. The resulting interaction strengths are slightly higher compared to previous satellite studies. The clusters which show large scale vertical movement, generally have higher interaction strengths.

CONTENTS

CHAPTER 1

INTRODUCTION

Earth receives energy from the Sun and in turn radiates energy away into space. The balance between incoming and outgoing radiation is called the Earth's Energy Balance or Earth's Energy Budget. Over long time periods and in a steady state situation, this balance will be in equilibrium and the Earth will have a constant temperature (Stephens et al, 2015).[1] Perturbations to the energy balance force the state to change. Perturbations can be natural or due to human (anthropogenic) activities. Examples of natural perturbations are injection of aerosols into the atmosphere by volcanic eruptions, changes in the orbit of the Earth, or a change in the energy output of the Sun. Perturbations due to anthropogenic activity are mainly emission of greenhouse gasses (CO_2, CH_4, etc) and aerosols (Joos & Spahni, 2008).[2] These perturbations induce a radiative forcing on the climate. Radiative forcing is the change in energy flux in the atmosphere due to a perturbation, measured in watts per square meter (Shindell et al, 2013).[3] Perturbations can cause a net positive or negative radiative forcing which causes a warming or cooling effect, respectively. A schematic representation of Earth's energy balance is shown in Figure 1.1.

To understand global warming it is crucial to study climate feedbacks. If the planet warms or cools due to a perturbation in the energy budget, the climate will respond, which can in turn cause an additional perturbation in the energy budget. Climate feedbacks as a response to global warming can thus amplify (positive feedback) or dampen (negative feedback) the warming (Stephens, 2005).[5] An example of a positive feedback is the water vapour feedback. As the temperature rises, more water vapour enters the atmosphere due to evaporation. This in turn causes additional heating, as water vapour is a strong greenhouse gas, which causes additional water vapour to enter the atmosphere.

Atmospheric aerosols have a big impact on the energy budget. Aerosols are particles in the atmosphere. Typical sizes range from 1 nanometer to 10 micron. The radii are distributed over different modes (nucleation, Aitken, accumulation, coarse, and more) (Schuster et al, 2006).[6] Aerosols can enter the atmosphere via two pathways. The resulting aerosols are called primary and secondary aerosols. Primary aerosols are emitted directly from a source, like sand, sea salt, or mineral dust. Secondary aerosols are formed in the atmosphere by a process called nucleation. Many different aerosols can form due to nucleation (Stephens et al, 2015).[1] A schematic representation of aerosol nucleation is shown in Figure 1.2. This process creates a range of possible aerosols with different compositions. Depending on the composition, atmospheric aerosols can act as Cloud Condensation Nuclei (CCN). CCN's are aerosols on which water can condensate to form a cloud droplet (Sun & Ariya, 2006).[7]

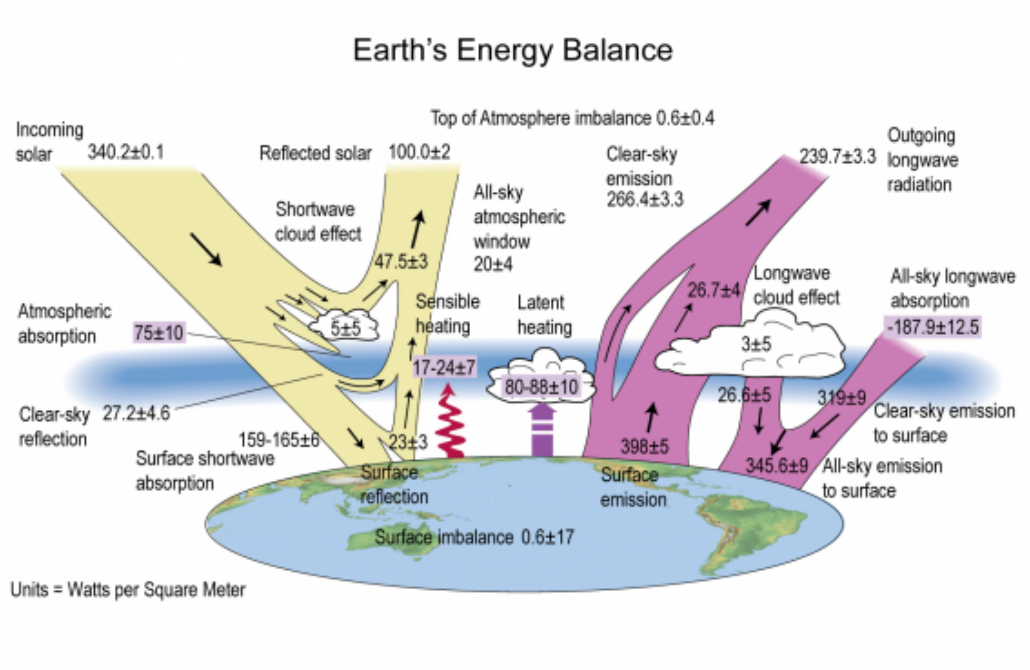

Figure 1.1: The Energy Balance of the Earth. The yellow arrows represent incoming and reflected solar irradiation which has short wavelengths (SW). The purple arrows indicate radiation emitted by the Earth which has longer wavelengths (LW). Sensible heat is the direct transfer of heat from the Earth's surface into the atmosphere by direct conduction. Latent heat is energy released by condensation of water as clouds form. The sum of all incoming and outgoing arrows should sum to zero, but there is a small imbalance which causes global warming. (Figure is modified from Stephens et al, 2012)[4]

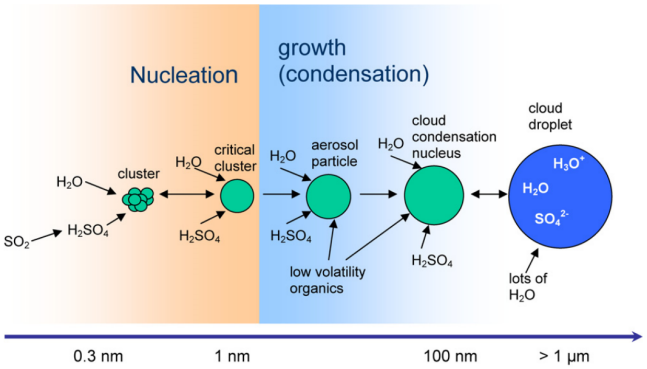

Figure 1.2: This figure shows nucleation of aerosols in the atmosphere. Molecules condensate and combine to form clusters that slowly grow. Under certain conditions the aerosol can act as a CCN and can form a cloud droplet. (Figure adopted from Curtius 2006)

Clouds absorb the Earth's infrared radiation and they reflect most solar irradiation, as shown in Figure 1.1. Consequently, they play a significant role in the total energy balance of the Earth. Small changes in the albedo of the clouds can significantly affect the global average albedo which in turn can significantly affect the climate (Somerville & Remer, 1984; Stephens et al, 1990)[8,9]. Different types of clouds exist at different altitudes which affect the climate differently. Which cloud types are able to form depends partly on the meteorology at a specific time. As the climate changes, clouds will adjust to the new situation which again changes the climate. Cloud-climate feedback is understood poorly and therefore making predictions about the future climate can be improved by studying clouds and their interactions.

1.1 Aerosol-Cloud Interactions

Aerosols have multiple effects on the climate that must be understood. The first is called the direct effect or aerosol radiation interaction (ARI). Aerosols in the atmosphere absorb and scatter incoming solar radiation. An increase in atmospheric aerosols gives rise to a net negative atmospheric forcing (Koch & Del Genio, 2010)[10] when considering only this effect. The radiative forcing of aerosol radiation interaction is denoted as RF_{ari}. The second effect is called the indirect effects or aerosol cloud interactions (ACI). There are multiple indirect effects and the primary indirect effect arises from aerosols acting as CCN. If the amount of CCN in a cloud increases, the amount of water droplets will be larger and the average size will be smaller, if the liquid water content (LWC), usually measured in $[g/m^3]$ or $[g/kg]$ (Bohren, 1998),[11] remains constant. The increased concentration of water droplets, increases the reflectivity of the cloud which has a negative radiative forcing in liquid clouds (Twomey, 1977),[12] denoted as RF_{aci}. The change in droplet number concentration and effective radius also changes the microphysics, properties, and lifetime of the cloud. All these effects are called the adjustments to ACI. An example of a negative forcing is the lifetime effect. As aerosols enter a precipitating cloud, the precipitation slows or stops as the droplets become smaller. This increases the lifetime of the cloud which allows it to reflect solar radiation longer. Figure 1.3 shows examples of cloud adjustments and how they induce a forcing. The radiative forcing of the direct effect combined with the adjustments is called the effective radiative forcing of aerosol cloud interactions ERF_{aci}. Measuring and predicting these effects has proven to be difficult and the Intergovernmental Panel on Climate Change (IPCC) has labelled aerosol-cloud interactions as the least well understood process in climate change science (IPCC AR6, WGI, Chapter 7).[13]

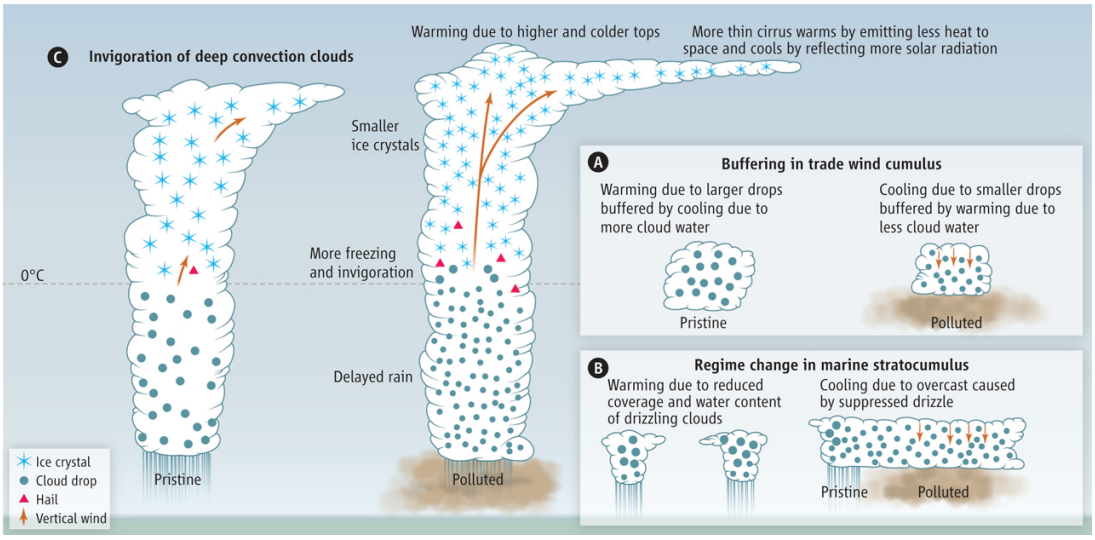

Figure 1.3: This figure shows cloud adjustments to increased aerosol concentrations (polluted clouds). A) Polluted clouds have more and smaller cloud droplets which increases evaporation. This causes more mixing with ambient air (orange arrows) which further increases evaporation. B) Precipitating clouds break up as they lose water droplets. This reduces cloud coverage. When these clouds have increased aerosol content, the precipitation is suppressed which can prevent clouds breaking up. C) Smaller droplets in a deep convective cloud allows the cloud to reach higher altitudes and have colder tops. Colder tops means less radiation emitted to space. This also produces more thin cirrus clouds that warm the planet. (Figure adapted from Rosenfeld et al. 2014)[14]

The relationship between the concentration of aerosols and the concentration of cloud droplets is used as a constraint to compute RF_{aci}. The slope of this relationship on a log-

log scale is referred to as the susceptibility (S). To compute the susceptibility from satellite measurements, a proxy for the amount of aerosols is required, as aerosol concentrations cannot be measured directly. In the past, Aerosol Optical Depth (AOD) (Quaas et al. 2009)[15] and Aerosol Index (AI) (Lohmann & Lesins, 2002)[16] were used, but Hasekamp et al. (2019)[17] showed that using a new proxy based on polarimetric observations produces results more inline with simulations and in-situ observations.

1.2 Regime based analysis

One path to better understand cloud adjustments are regime based studies. Gryspeerdt & Stier (2012)[18] show the importance of studying aerosol-cloud interactions in different regimes, due to the different interaction strengths. They find different regimes by clustering cloud properties. Scott et al. (2020)[19] showed that by classifying regimes based on meteorological parameters, the evaluation of marine low-cloud feedback can be better understood. This in turn can improve climate models. Mülmenstädt & Feingold (2018)[20] mention that:

> [Studying aerosol effects by subsampling data by cloud controlling metrics] would help limit the meteorological parameter space, defining distinct cloud regimes and, hence, reduce the number of degrees of freedom in the system. *-Mülmenstädt & Feingold (2018)[20]*

However, they also mention that meteorological metrics are imperfect and difficult to classify, because small differences matter. As the relation between aerosol and clouds is related to the cloud regime, and thus also related to the meteorology, studying aerosol-cloud interactions per meteorological regime is an interesting research path. Modern clustering techniques allow for fast pattern recognition in data and have proven to be useful and applicable in climate science (i.e. Gryspeerdt & Stier 2012;[18] Evans et al. 2012;[21] Abraham & Goldblatt, 2022[22]).

In the next chapter, the methodology of this research is explained. In Chapter 3 the results are presented. In Chapter 4 the findings are summarised and discussed.

CHAPTER 2

METHODOLOGY

In this chapter we discuss the methodology of the research. We first describe the data that is used, and then we discuss the clustering techniques and how the susceptibilities are computed.

2.1 Data description

Three data sets are used in this study. All data is restricted to 2006. Furthermore we only use pixels over the ocean and latitudes between 60°S and 60°N because the quality of the aerosol retrievals is the highest in these locations. The aerosol products are retrievals from POLDER-3 data using the SRON aerosol retrieval algorithm (Hasekamp et al. 2011,2019; Stap et al. 2015)[23,17,24] . We use CCN concentrations which are derived from the retrieved number concentrations of spherical aerosols with $r > 0.15$ micron. Hasekamp et al. (2019) showed that this measure of aerosol concentrations produces more realistic estimates of the susceptibility. The cloud droplet number concentration (CDNC) is computed from the MODIS Collection-6 retrievals of droplet effective radii and optical thickness (Grosvenor et al. 2018).[25] See Hasekamp et al. (2019) for more details on the aerosol and CDNC retrievals.

To find meteorological clusters, data from the Modern-Era Retrospective analysis for Research and Applications, Version 2 (MERRA-2), is used (GMAO, 2015).[26] The reanalysis data computes a range of different parameters at 42 different pressure levels. The parameters we use to cluster the meteorology are surface temperature ($T_{surface}$), surface wind-speed ($UV_{surface}$), Lower Tropospheric Stability (LTS), and lastly, relative humidity (RH) and pressure vertical velocity (Ω) at the 700 and 500 hPa pressure level. The surface wind-speed is computed by taking the root sum squared of the U and V direction of the wind (westerly and southerly wind). Thus we lose the directional component and only have the magnitude in the U-V plane. LTS is a measure of atmospheric stability and is defined as the difference between the potential temperature (q) of the free troposphere (700 hPa) and the surface, see Equation 2.1 (Klein & Hartmann, 1993).[27] We can use LTS as a proxy for cloud cover, as LTS is highly correlated with cloud fraction (CF) (Wood & Bretherton, 2006)[28] .

$$LTS = q_{700} - q_0 = T_{700}\left(\frac{P_0}{P_{700}}\right)^{R/c_p} - T_0\left(\frac{P_0}{P_0}\right)^{R/c_p} = T_{700}\left(\frac{P_0}{P_{700}}\right)^{R/c_p} - T_0. \tag{2.1}$$

The MERRA-2 data is computed on a grid of 0.5° latitude by 0.625° longitude every three hours. The cloud and aerosol retrievals are computed on a grid of 1° latitude by 1° longitude.

The retrieval time depends on the orbital parameters. The satellites pass the equator at around 13 : 30 local time. For this research we assume that all measurements are taken at 13 : 30 local time instead of accounting for the orbit. The conversion to UTC is then done by using the following relation:

$$UTC = t_{local} + \frac{lon}{15}. \tag{2.2}$$

For the spatial reprojection we choose the nearest neighbour to reproject Merra-2 onto the satellite retrieval grid. For the temporal reprojection we compute the local time at each 1° by 1° grid point and interpolate the closest two temporal points in the Merra-2 data to the local time. For the surface wind-speed and temperature we also interpolate the pressure levels to the surface pressure.

2.2 Clustering

To find clusters in the meteorological data, the k-means clustering algorithm is used (Saxena et al. 2017).[29] Other options have been considered (Fuzzy C-Means, DBSCAN, Optics), but k-means is chosen due to the flexibility and scalability of the algorithm. The aim of the algorithm is to partition the data as to minimise the variance within a cluster. See Saxena et al. (2017)[29] for an overview of clustering techniques.

To find the optimum number of clusters an elbow plot and different cluster metrics are used. Figure 2.1 shows the elbow plot. Each point is the mean of 1000 clustering runs. Inertia or within-cluster sum-of-squares (or simply the variance) is a measure of how coherent a cluster is. The algorithm chooses centroids that minimise the following expression:

$$\sum_{i=0}^{n} \min_{\mu_j \in C} \left(\|x_i - \mu_j\|^2 \right), \tag{2.3}$$

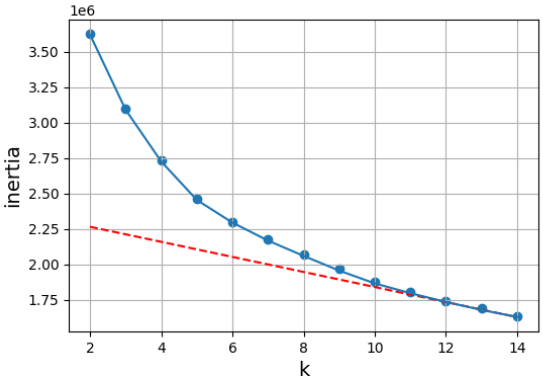

Figure 2.1: Elbow plot to estimate the optimal number of clusters.

where μ_i is the centre of the cluster i and x_j is point j in cluster i (Bock, 2007).[30] The inertia reduces as the amount of clusters (k) increases. In the limit of k approaching the number of points (k→ N) the inertia will approach zero. The elbow of an elbow plot is the point where the slope significantly flattens. From the figure no clear elbow point can be found, but by drawing a straight line through the last two points we choose k=8 for this analysis. This choice is somewhat arbitrary, and we have tried and visualised all possibilities from k=3 to k=12 and eventually chose k=8 for this thesis.

To test the stability of the clusters, the clustering was performed multiple times with different random initialisations. No apparent difference could be found, indicating that a global minimum is found.

2.3 Susceptibility of clouds to aerosol perturbations

The formula for the susceptibility of cloud droplet number concentrations to CCN concentrations is:

$$S = \frac{d \log N_d}{d \log N_{ccn}}. \tag{2.4}$$

To compute the susceptibilities from the POLDER-3 and MODIS data, we first match the clustered MERRA-2 data to the satellite retrievals. Then for every unique cluster in the dataset we select only the grid cells where there are both N_d and N_{ccn} retrievals. Then, for each cluster, we define 20 bins for N_{ccn} with equal numbers of data points and we find the corresponding N_d and N_{ccn} values for those bins by computing the median of the points in the bin. Then we compute the susceptibility by doing a linear Least-Squares fit of the median values in log-log space. Following Hasekamp et al. (2019),[17] we only consider points with $N_{ccn} > 10^7$, as including lower values leads to an underestimation of S due to estimation errors. Increasing the number of bins has no substantial effect on the computed slope.

CHAPTER 3

RESULTS

This chapter is split up in two parts. First we describe the clusters based on the meteorological parameters. Then we look at the aerosol cloud interactions per cluster.

3.1 Cluster descriptions

Figure 3.1 shows a box-plot of the meteorological parameters and latitude/longitude per cluster. Note that the latitude/longitude were not used for clustering, but were added for

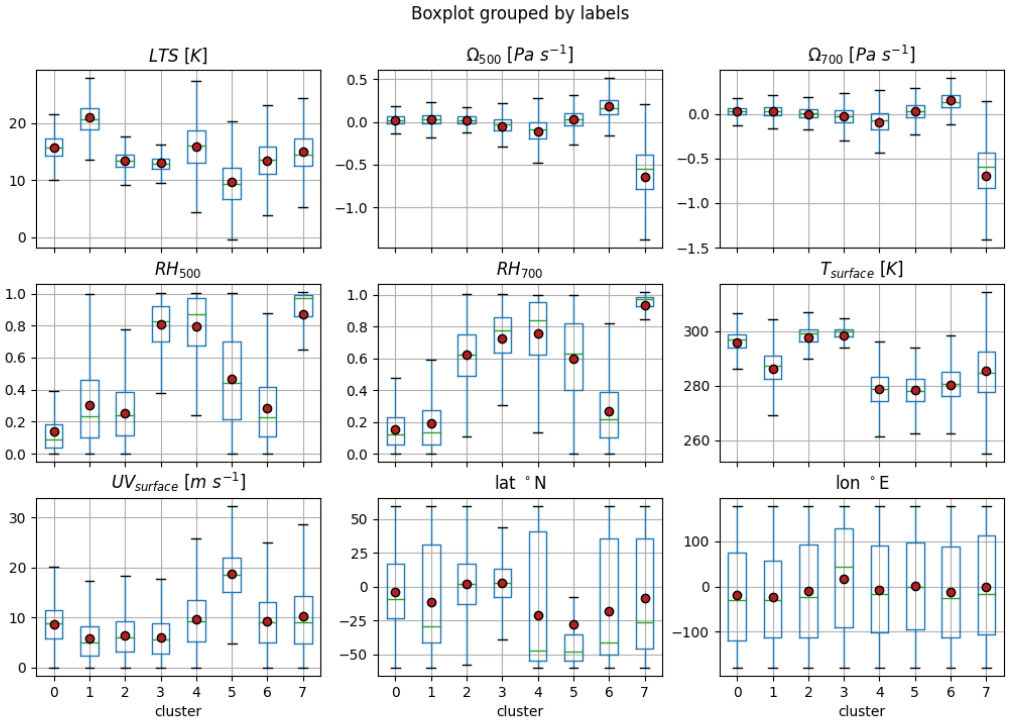

Figure 3.1: A box plot of the meteorological parameters per cluster. Latitude and longitude are also shown but these were not used in the clustering process. The boxes and the green line represent the 25%, 50% and 75% quantiles, and the red dot indicates the mean. The whiskers show the range of the data.

Number	Name	Number of points	Cluster characteristics
0	Trade Wind Cumulus	2710242 (23.4%)	Low RH at 700 and 500 hPa, near equator
1	Stratiform Cumulus	1746099 (15.0%)	High LTS, low RH, low UV_s, coastal
2	Weak Hadley Movement	1997889 (17.2%)	High RH at 700 hPa, low RH at 500 hPa, equator
3	Tropical Convection	1793753 (15.5%)	High RH at 700 and 500 hPa, high T, equator
4	Moist mid-latitude winds	1208047 (10.4%)	High RH, mid-latitudes,
5	Mid-latitude winds	963249 (8.3%)	High UV_s, mid-latitudes,
6	Mid-latitude convection	957931 (8.3%)	Positive Ω, mid-latitudes
7	Ω outliers	229425 (2.0%)	High RH, negative Ω values

Table 3.1: The different clusters are listed. As are their names, the number of points per cluster, and some characteristics.

reference. The edges of the box represent the 25% and 75% quantiles, the green line represents the 50% quantile or median, and the red dot represents the mean. The whiskers show the range of the data, excluding outliers. Only data within $1.5 \cdot (Q3 - Q1)$ from the edges of the box are considered, so points beyond this range are labelled outliers. Each cluster has unique characteristics. We will analyse the clusters per characteristics group and we will refer to the clusters as C0, C1, etc. or by their name defined above.

In Table 3.1, the cluster number, cluster name, number of points, and some characteristics are shown. The names are chosen based on literature studies (Scott et al, 2020; Gryspeerdt et al, 2012; Abraham & Goldblatt, 2022), but they are not exact. They give an approximate sense of the clustered meteorology or the resulting cloud formations.

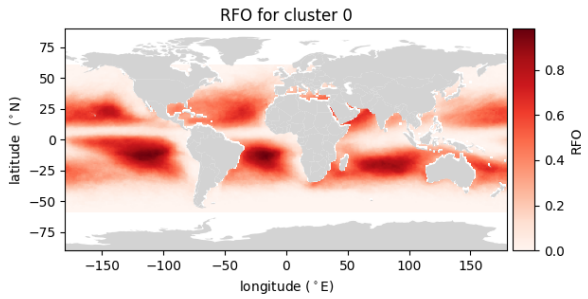

Figure 3.2: RFO of C0, or Trade Wind Cumulus

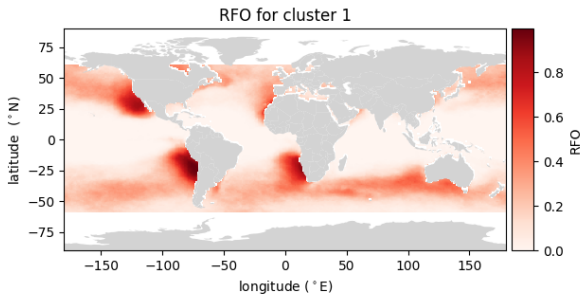

Figure 3.3: RFO of C1, or Stratiform Cumulus

Cluster 0 and 1 are called 'Trade Wind Cumulus' and 'Stratiform Cumulus', respectively. Figure 3.2 and Figure 3.3 show the relative frequency of occurrence (RFO) per pixel for C0 and C1. Both clusters are concentrated around the equator. The Trade Wind Cumulus cluster lie

over the open oceans, while C1 points primarily lie close to the west coasts of America and Africa. Both clusters have low RH, except that C1 has somewhat higher RH values at 500 hPa. C1 has high LTS and low wind-speed. C1 contain areas of high cloud cover, as LTS is strongly correlated with cloud fraction (CF) (Wood & Bretherton, 2006).[28] C0 has somewhat higher wind speeds, which can be attributed to the higher wind speeds over the ocean. The low RH values of C0 could be caused by dry air coming from the continents.

Cluster 2 and 3 are both concentrated around the equator. They are called 'Weak Hadley Movement' and 'Tropical Convection' respectively. The Weak Hadley Movement cluster shows low RH at 500 hPa and high RH at 700 hPa. This indicates moist near surface conditions, which decreases with increasing altitude. Looking at the spatial distribution of C2 (Figure 3.4), we see high concentrations near the equator and some points around lower and higher latitudes. The Tropical Convection cluster has high RH at both 500 and 700 hPa and higher spread in Ω. This indicates that near-surface moisture is able to rise and be transported higher into the troposphere, compared to the Weak Hadley Movement regime. The higher spread in Ω shows that there is large scale upward and downward motion. All these grid cells could potentially contain combinations of cumulus, congestus and deep convective cloud formations, so the name 'Tropical Convection' does not indicate that these grid cells primarily contain deep convective clouds.

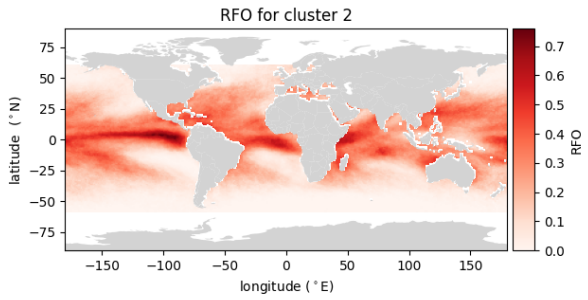

Figure 3.4: RFO of C2, or Weak Hadley Movement

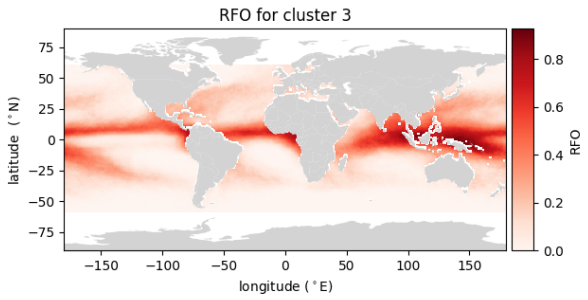

Figure 3.5: RFO of C3, or Tropical Convection

Cluster 4 and 5 are called 'Moist mid-latitude winds' and 'Mid-latitude winds' respectively. Both clusters are concentrated around the mid-latitudes (Figure 3.6, Figure 3.7), and show higher wind-speeds compared to other clusters. C4 has mostly high values for RH at both pressure levels, while the mean RH of C5 lies around 50% with a spread over the entire domain. The Moist-mid-latitude regime shows high values in LTS. This indicates that there is expected to be high CF in this cluster. C5 has the highest wind-speeds and the lowest LTS (which translates to low expected CF). This cluster also has a high concentration above the Southern part of the Indian Ocean where there are strong wind currents.

Cluster 6 and 7 show significant high and low values in Ω at both pressure levels. C6 is called 'mid-latitude convection' and is characterised by positive Ω and low RH. Spatially, the cluster is primarily located in the mid-latitudes (Figure 3.8. From this we can conclude that this is likely associated with the downward motion of the Hadley circulation cells. C7 is called 'Ω outliers', as the cluster includes extreme low values of Ω and the cluster is quite empty (2% of the points). Looking at the spatial distribution (Figure 3.9), we see that the points lie evenly distributed, but there are a few points of high concentration near land-ocean boundaries.

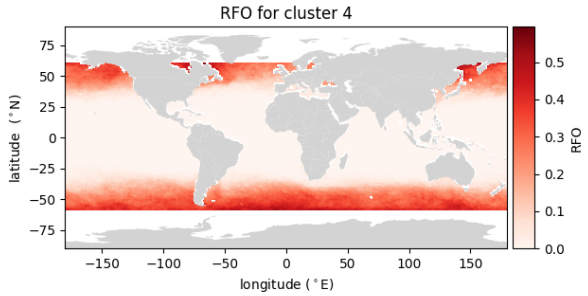

Figure 3.6: RFO of C4, or Moist mid-latitude winds

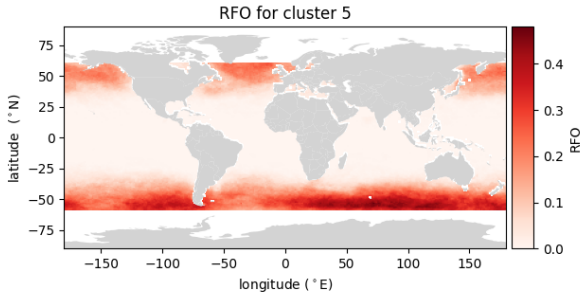

Figure 3.7: RFO of C5, or Mid-latitude winds

Particularly near Taiwan, Chile, and Colombia. These points also have very high RH. These are points with very large upward motion.

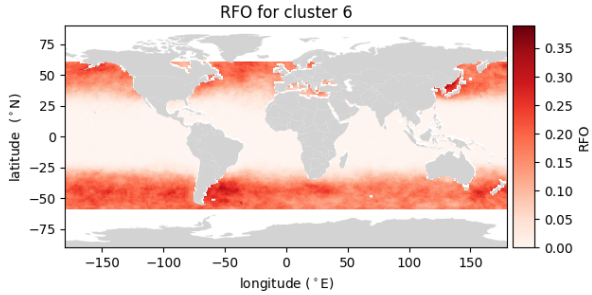

Figure 3.8: RFO of C6, or Mid-latitude convection

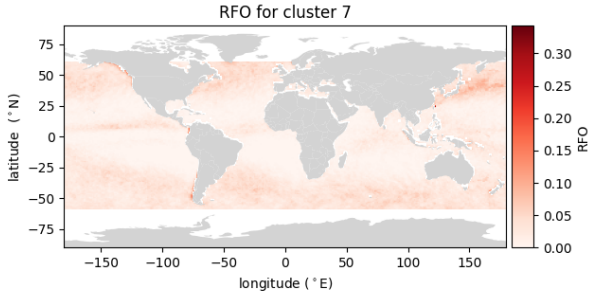

Figure 3.9: RFO of C7, or Ω outliers

In the Appendix , the seasonal variation of all the clusters are shown. All the clusters show some seasonal pattern. Some clusters are more prevalent in the summer while others are more prevalent in the winter.

3.2 Susceptibilities

Table 3.2 shows the percentage of the points per cluster that have an aerosol and a cloud retrieval from the satellite data. The Weak Hadley Movement, Tropical Convection, and Mid-latitude Winds clusters have relatively low amounts of retrievals. This could be partly explained by ice cloud formations in deep convective clouds which impede cloud droplet retrievals. These clusters also have low LTS, which translates to low CF. This could indicate that that there are relatively many broken cloud formations, which make aerosol and cloud retrievals more difficult (See Grosvenor et al. 2018).[25]

Figure 3.10 and Figure 3.11 show the binned data and the two linear regressions to those binned points. The legend shows the number of points and the value of the slope with the least-squares estimation error. Both plots have about the same susceptibility. Cluster 0 has

Number	Name	Percentage of points with retrievals
0	Trade Wind Cumulus	40%
1	Stratiform Cumulus	37%
2	Weak Hadley Movement	34%
3	Tropical Convection	34%
4	Moist mid-latitude winds	40%
5	Mid-latitude winds	35%
6	Mid-latitude convection	40%
7	Ω outliers	42%

Table 3.2: The percentage of points per cluster that have an aerosol and cloud retrieval.

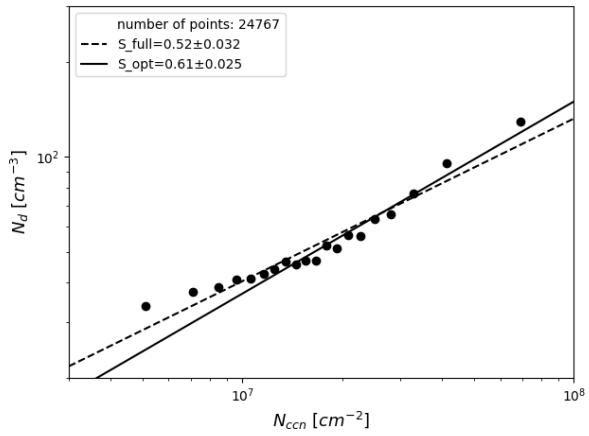

Figure 3.10

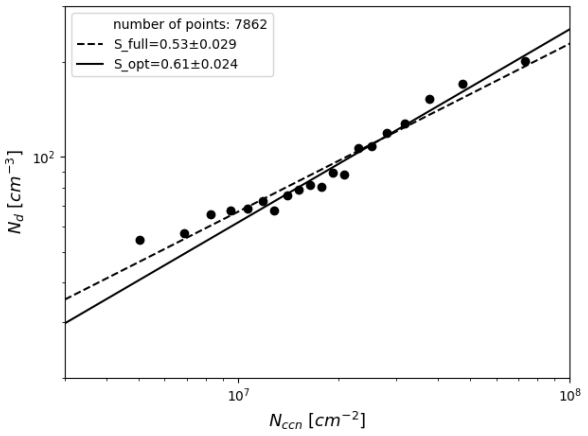

Figure 3.11

much more data points which can also be seen in Table 3.2. The points in Figure 3.11 lie significantly higher on the graph compared to Figure 3.10. This indicates that for the same aerosol perturbation there is a different response in CDNC. This indicates that the meteorology has an effect on if a cloud droplet can form, as C1 differs significantly from C0 in temperature and LTS. The lower temperature and higher LTS could indicate that cloud droplets can form more easily. Another explanation could be drop loss due to precipitation (See Jia et al. 2022).[31]

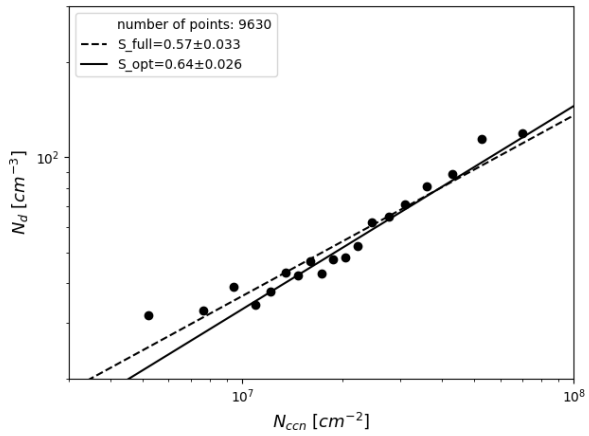

Figure 3.12

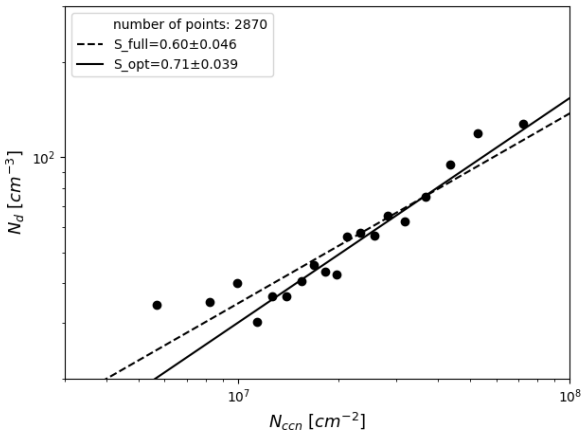

Figure 3.13

Figure 3.12 and Figure 3.13 show the fits for cluster 2 and cluster 3, which were both spatially distributed around the equator. C2, or the Weak Hadley Movement regime, shows a

comparable value to the first two clusters. This indicates that these meteorological conditions produce about the same strength of aerosol-cloud interactions. C3, or the Tropical Convection regime, has a higher value for the susceptibility. This is an indication that vertical movement has an effect on aerosol-cloud interactions and that there are circumstances around the equator where there are strong aerosol-cloud interactions.

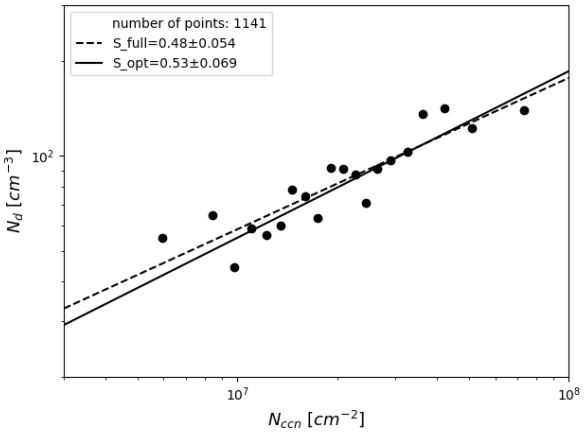

Figure 3.14

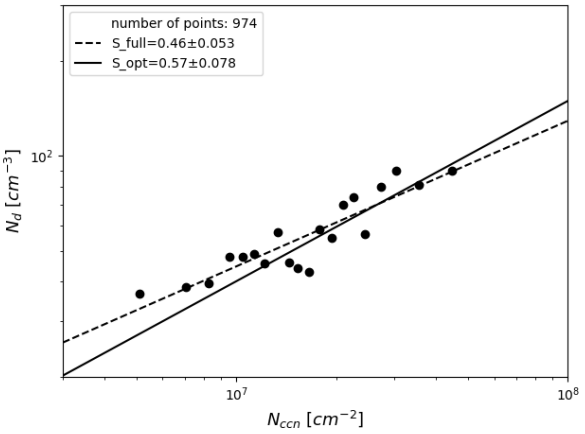

Figure 3.15

C4 and C5 both have somewhat lower values for S, as can be seen in Figure 3.14 and Figure 3.15, but the error is quite large due to the low amount of points in this cluster. It can be seen that C4 lies higher on the graph while C5 lies lower on the graph. These mid-latitude regimes with relatively high wind-speeds have weaker aerosol-cloud interactions.

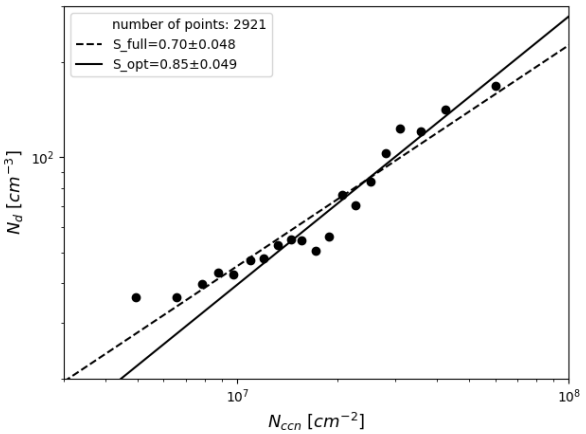

Figure 3.16

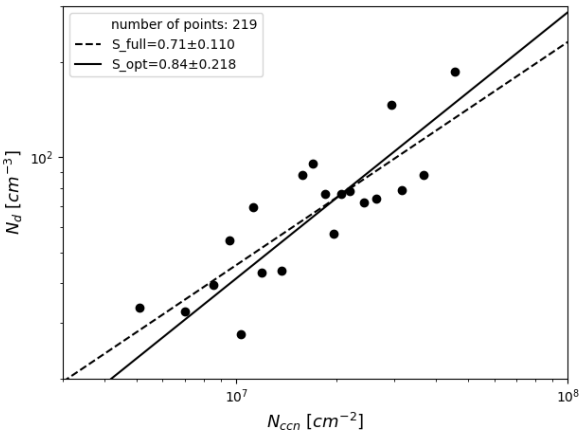

Figure 3.17

C6 has a very high value of S (Figure 3.16). The same value can be seen for C7 (Figure 3.17), but the size of the cluster is very small, which causes the extremely high uncertainty. These two cluster have the highest and lowest values of Ω, indicating that there is large scale upward and downward motion. Interestingly, when there is large scale downward motion, the ACI are still very strong. The Ω values are averaged over a large grid box, so it is possible that there is also upward motion in the grid box when Ω is positive, which indicates downward motion.

Figure 3.18 shows the relationship between N_d and N_{ccn} for all clusters. The legend shows the computed susceptibilities with the least-squares error.

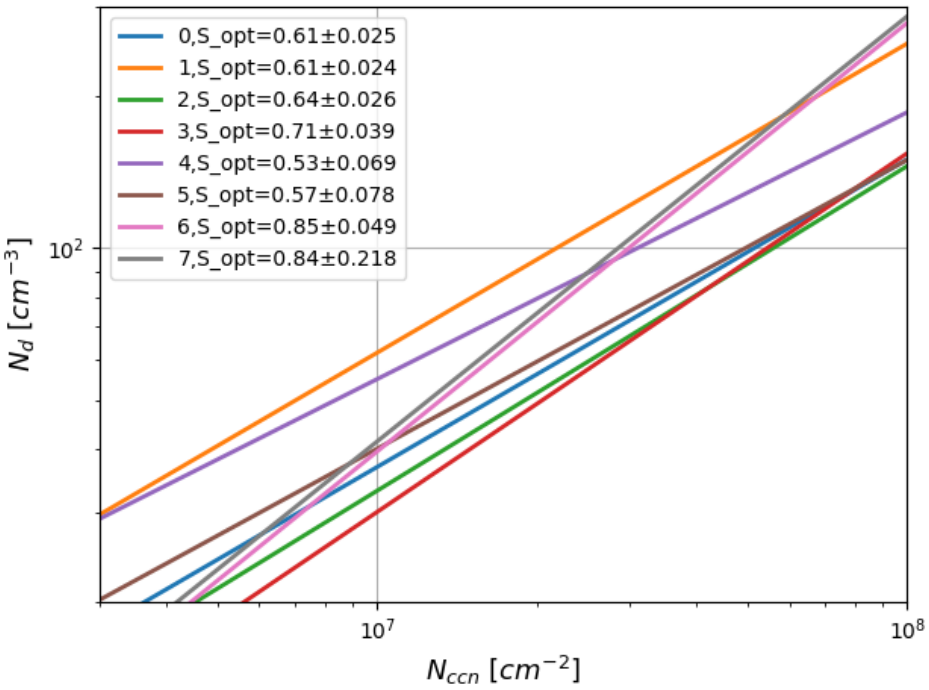

Figure 3.18: The computed least-squares fit to the binned satellite retrievals per cluster. The susceptibilities and the least-squares error are shown in the legend.

CHAPTER 4

DISCUSSION

Regime based studies are crucial for improving understanding of aerosol-cloud interactions. This thesis demonstrates the possibility of studying the variation in ACI strength by meteorological clustering. Using the k-means clustering algorithm we identified 8 clusters in one year of MERRA-2 reanalysis data over oceans. All clusters have a specific fingerprint in the meteorological parameters, but they are not well-seperated. This is caused by the uniform nature of the data. The clusters show spatial patterns comparable to other studies (Evans et al. 2012; Abraham & Goldblatt, 2022)[21,22] . Clusters were given names corresponding to the meteorology or possible cloud formation in that cluster.

For the resulting clusters we computed the susceptibility of cloud droplet number concentrations with respect to cloud condensation nuclei concentrations, S, using MODIS cloud and POLDER-3 aerosol satellite data. The susceptibilities range from 0.53 to 0.85. These values lie within the range of the IPCC significant range. Satellite remote sensing estimates of S are usually lower compared to airborne measurements (Schmidt et al. 2015).[32] This is partly caused by the limitations of satellite observations (Quaas et al. 2020).[33] One such limitation is the fact that aerosol satellite retrievals are made next to the clouds (Gryspeerdt et al. 2015).[34] We want to measure the concentrations below the clouds, but that is not possible due to cloud obscuring the atmosphere below. Furthermore, the clouds scatter solar radiation which increases uncertainty in the estimation of aerosol concentrations. McComiskey and Feingold (2012)[35] also argue that the main reason for the low values of S for satellite estimates is probably that the analysis scale is larger than the process scale. Aerosols affect clouds at cloud droplet scales while satellites capture bulk properties over a large area. Overcoming the scale problem is an important aspect of ACI quantification. Hasekamp et al. (2019)[17] computed S for different geographical regimes with the same data used here. Comparing our values to these values shows that our values lie within the same range, but are less extreme on the low side. Their lowest value is 0.44 while ours is 0.53.

The highest values of S are found in the clusters where the large scale vertical movement (Ω) is high or low. This could be explained by the fact that when there is a lot of vertical movement in the atmosphere, higher levels of supersaturation can be reached and more aerosols are able to act as CCN. However, Ω only measures large scale movement. All the fine scale upward and downward motions are not captured, so it is impossible to make statements about the finer scale physics happening in a grid cell. Jia et al. (2022)[31] show that there is a strong scaling between S and vertical velocity at cloud base, but the exact impact on S needs to be assessed.

Precipitating clouds introduce a bias in the computed susceptibility (Jia et al. 2022).[31] By not accounting for this, some of our susceptibilities might be biased too high. Precipitating clouds would have lower N_d retrievals, as cloud droplets are falling to the ground. This means that especially the clusters with low values of N_d could be biased. This could affect the Trade Wind Cumulus, Weak Hadley Movement, Tropical Convection, and Mid-Latitude Winds regimes. This analysis could be improved by adjusting for this effect. Precipitating clouds would need to be detected using satellite observations (Kenneth et al. 2021; Dzambo et al. 2021)[36,37] .

The k-means algorithm is sensitive to outliers (Saxena et al. 2017).[29] We saw that one cluster contained most extremely negative values of Large Scale Vertical movement (Ω). These points could be an artefact of the retrieval algorithms on the land-ocean boundary. A clustering method that detects outliers could prove useful in clustering meteorological data. Using an algorithm like DBSCAN or a fuzzy clustering algorithm might provide better clustering results. Both of these types of clustering algorithms are able to detect outliers.

Using the values for S per regime, the radiative forcing of aerosol-cloud interactions RF_{aci} can be computed. Using regime based values for S should give a more realistic estimate of RF_{aci}. The approach of Hasekamp et al. (2019)[17] can be applied here to produce an estimate. Another interesting possibility is applying such an analysis on model data, to see if the model produces the same results. A complication is that the model would need to compute the same meteorological parameters that we used for the clustering. When the new satellite PACE (Plankton, Aerosol, Cloud, ocean Ecosystem) will be launched, more precise aerosol and cloud retrievals can be made using the instruments on board. PACE will also be able to measure aerosols over land which is not possible with POLDER-3 data. Using these new retrievals, this analysis can be reproduced to improve the estimate of the susceptibility and thus improve the estimate of the radiative forcing.

Improving our estimate of the radiative forcing of aerosol-cloud interactions is crucial to further out knowledge of climate change. Considering different meteorological regimes allows better estimation, but there are a plethora of methods for defining the regimes. We have shown that a simple approach can already produce interesting results.

Appendix

Seasonal variation

Below are histograms of the occurrences of each clusters per season. Every cluster shows some dependency on season as the seasons affect the meteorology. Some clusters prefer winter while others prefer summer.

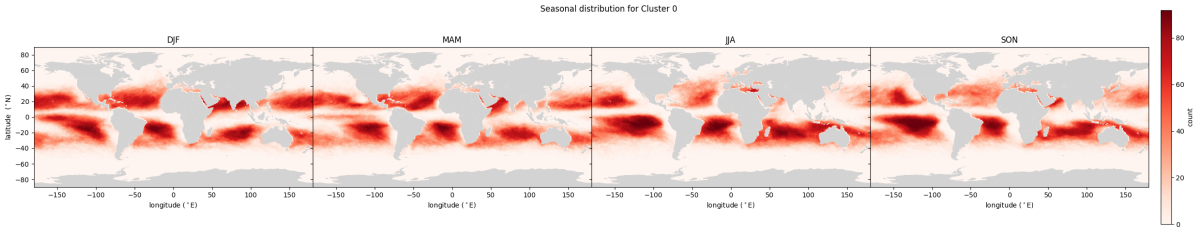

Figure 4.1: Seasonal variation of cluster 0

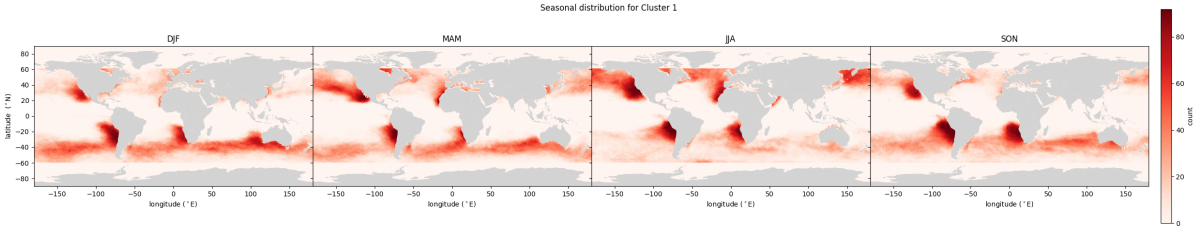

Figure 4.2: Seasonal variation of cluster 1

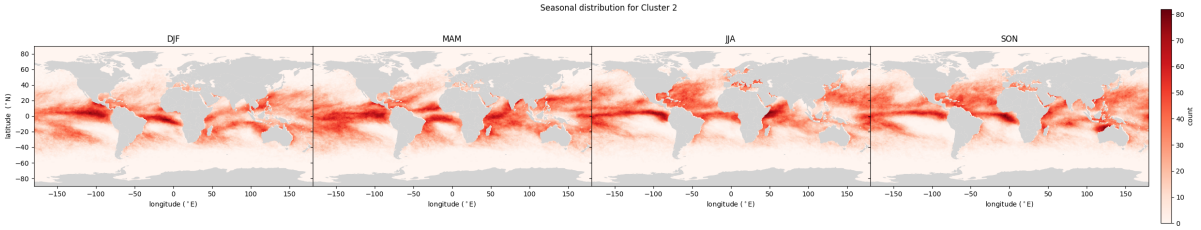

Figure 4.3: Seasonal variation of cluster 2

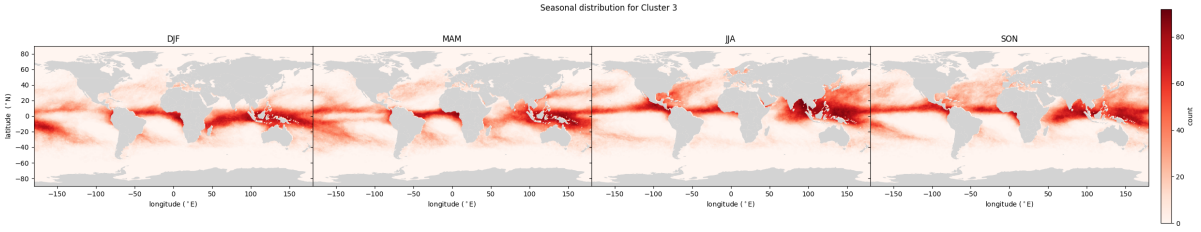

Figure 4.4: Seasonal variation of cluster 3

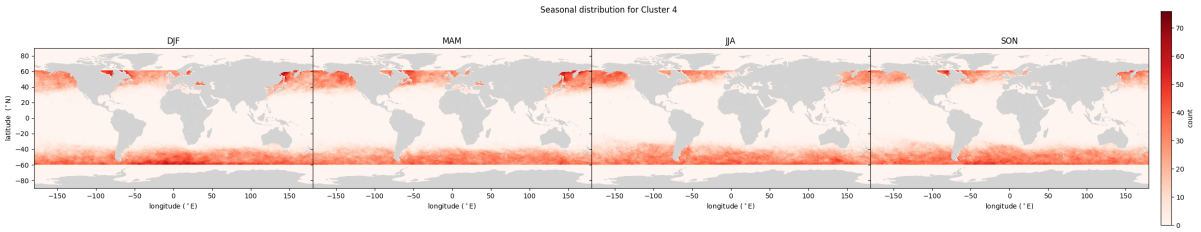

Figure 4.5: Seasonal variation of cluster 4

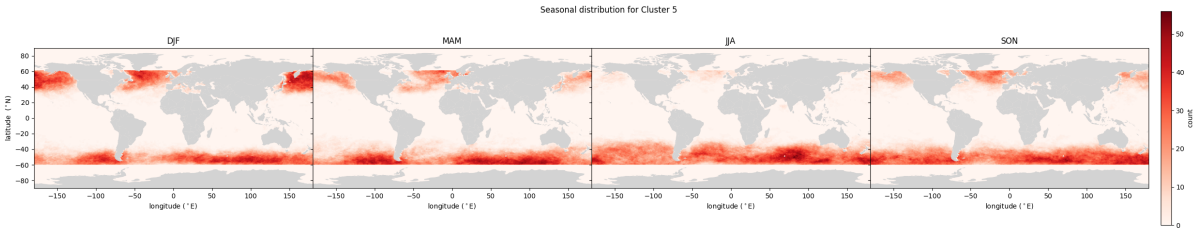

Figure 4.6: Seasonal variation of cluster 5

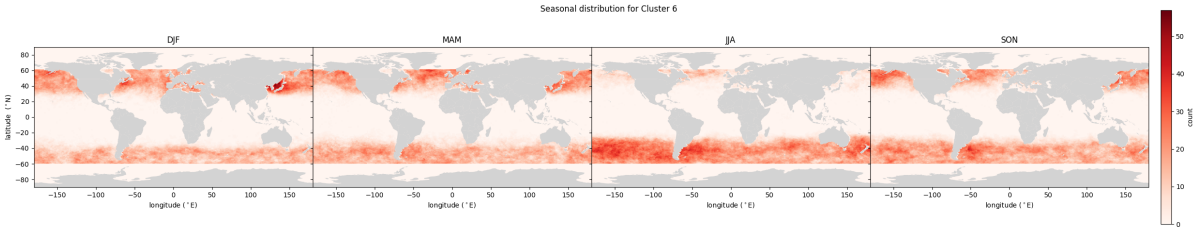

Figure 4.7: Seasonal variation of cluster 6

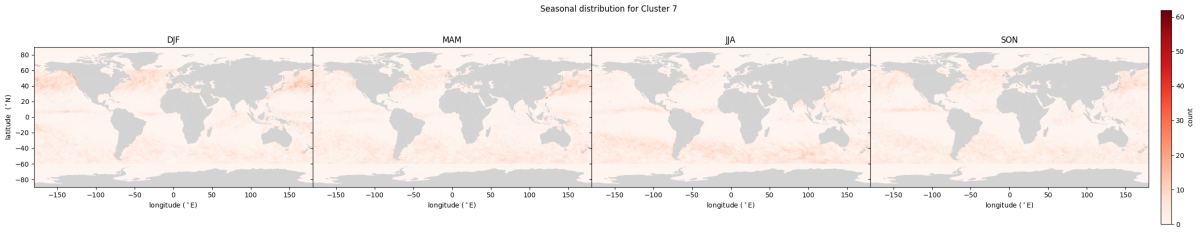

Figure 4.8: Seasonal variation of cluster 7

BIBLIOGRAPHY

[1] Stephens, G. L. *et al.* The albedo of earth. *Reviews of Geophysics* **53**, 141–163 (2015). URL https://agupubs.onlinelibrary.wiley.com/doi/abs/10.1002/2014RG000449.

[2] Joos, F. & Spahni, R. Rates of change in natural and anthropogenic radiative forcing over the past 20,000 years. *Proceedings of the National Academy of Sciences of the United States of America* **105**, 1425–1430 (2008).

[3] Shindell, D. T. *et al.* Radiative forcing in the accmip historical and future climate simulations. *Atmospheric Chemistry and Physics* **13**, 2939–2974 (2013). URL https://acp.copernicus.org/articles/13/2939/2013/.

[4] Stephens, G. L. *et al.* An update on Earth's energy balance in light of the latest global observations. *Nature Geoscience* **5**, 691–696 (2012).

[5] Stephens, G. L. Cloud feedbacks in the climate system: A critical review. *Journal of Climate* **18**, 237 – 273 (2005). URL https://journals.ametsoc.org/view/journals/clim/18/2/jcli-3243.1.xml.

[6] Schuster, G. L., Dubovik, O. & Holben, B. N. Angstrom exponent and bimodal aerosol size distributions. *Journal of Geophysical Research: Atmospheres* **111** (2006). URL https://agupubs.onlinelibrary.wiley.com/doi/abs/10.1029/2005JD006328.

[7] Sun, J. & Ariya, P. A. Atmospheric organic and bio-aerosols as cloud condensation nuclei (CCN): A review. *Atmospheric Environment* **40**, 795–820 (2006). URL https://www.sciencedirect.com/science/article/pii/S135223100500498X.

[8] Somerville, R. C. & Remer, L. A. Cloud optical thickness feedbacks in the CO2 climate problem. *Journal of Geophysical Research* **89**, 9668–9672 (1984). URL https://agupubs.onlinelibrary.wiley.com/doi/abs/10.1029/JD089iD06p09668.

[9] Stephens, G. L., Tsay, S.-C., Stackhouse, P. W. & Flatau, P. J. The relevance of the microphysical and radiative properties of cirrus clouds to climate and climatic feedback. *Journal of Atmospheric Sciences* **47**, 1742 – 1754 (1990). URL https://journals.ametsoc.org/view/journals/atsc/47/14/1520-0469_1990_047_1742_trotma_2_0_co_2.xml.

[10] Koch, D. & Del Genio, A. Black carbon semi-direct effects on cloud cover: review and synthesis. *Atmospheric Chemistry and Physics* **10**, 7685–7696 (2010).

[11] Bohren, C. F. & Albrecht, B. A. *Atmospheric thermodynamics* (Oxford University Press, 1998).

[12] Twomey, S. The Influence of Pollution on the Shortwave Albedo of Clouds. *Journal of Atmospheric Sciences* **34**, 1149–1152 (1977). URL https://journals.ametsoc.org/view/journals/atsc/34/7/1520-0469_1977_034_1149_tiopot_2_0_co_2.xml.

[13] Forster, P. *et al.* The Earthâs Energy Budget, Climate Feedbacks, and Climate Sensitivity. In Masson-Delmotte, V. *et al.* (eds.) *Climate Change 2021: The Physical Science Basis. Contribution of Working Group I to the Sixth Assessment Report of the Intergovernmental Panel on Climate Change*, chap. 7 (Cambridge University Press, Cambridge, United Kingdom and New York, NY, USA, 2021). URL https://www.ipcc.ch/report/ar6/wg1/downloads/report/IPCC_AR6_WGI_Chapter_07.pdf.

[14] Rosenfeld, D., Sherwood, S., Wood, R. & Donner, L. Climate effects of aerosol-cloud interactions (2014).

[15] Quaas, J. *et al.* Aerosol indirect effects-general circulation model intercomparison and evaluation with satellite data. *Atmospheric Chemistry and Physics* **9**, 8697–8717 (2009).

[16] Lohmann, U. & Lesins, G. Stronger constraints on the anthropogenic indirect aerosol effect. *Science* **298**, 1012–1015 (2002).

[17] Hasekamp, O. P., Gryspeerdt, E. & Quaas, J. Analysis of polarimetric satellite measurements suggests stronger cooling due to aerosol-cloud interactions. *Nature Communications* **10**, 1–7 (2019). URL http://dx.doi.org/10.1038/s41467-019-13372-2.

[18] Gryspeerdt, E. & Stier, P. Regime-based analysis of aerosol-cloud interactions. *Geophysical Research Letters* **39**, 1–5 (2012).

[19] Scott, R. C. *et al.* Observed sensitivity of low-cloud radiative effects to meteorological perturbations over the global oceans. *Journal of Climate* **33**, 7717–7734 (2020).

[20] Mülmenstädt, J. & Feingold, G. The Radiative Forcing of AerosolâCloud Interactions in Liquid Clouds: Wrestling and Embracing Uncertainty (2018).

[21] Evans, S. M., Marchand, R. T., Ackerman, T. P. & Beagley, N. Identification and analysis of atmospheric states and associated cloud properties for Darwin, Australia. *Journal of Geophysical Research Atmospheres* **117**, 1–12 (2012).

[22] Abraham, C. & Goldblatt, C. A satellite climatology of relative humidity profiles and outgoing thermal radiation over Earthâs oceans. *Journal of the Atmospheric Sciences* **79**, 2243–2265 (2022).

[23] Hasekamp, O. P., Litvinov, P. & Butz, A. Aerosol properties over the ocean from PARASOL multiangle photopolarimetric measurements. *Journal of Geophysical Research Atmospheres* **116**, 1–13 (2011).

[24] Stap, F. A., Hasekamp, O. P. & Röckmann, T. Sensitivity of PARASOL multi-angle photopolarimetric aerosol retrievals to cloud contamination. *Atmospheric Measurement Techniques* **8**, 1287–1301 (2015). URL https://amt.copernicus.org/articles/8/1287/2015/.

[25] Grosvenor, D. P. *et al.* Remote sensing of droplet number concentration in warm clouds: A review of the current state of knowledge and perspectives. *Reviews of Geophysics* **56**, 409–453 (2018). URL https://agupubs.onlinelibrary.wiley.com/doi/abs/10.1029/2017RG000593. https://agupubs.onlinelibrary.wiley.com/doi/pdf/10.1029/2017RG000593.

[26] Global Modeling And Assimilation Office & Pawson, S. MERRA-2 inst3_3d_asm_Np: 3d, 3-Hourly, Instantaneous, Pressure-Level, Assimilation, Assimilated Meteorological Fields V5.12.4 (2015). URL https://disc.gsfc.nasa.gov/datacollection/M2I3NPASM_5.12.4.html.

[27] Klein, S. A. & Hartmann, D. L. The seasonal cycle of low stratiform clouds. *Journal of Climate* **6**, 1587 – 1606 (1993). URL https://journals.ametsoc.org/view/journals/clim/6/8/1520-0442_1993_006_1587_tscols_2_0_co_2.xml.

[28] Wood, R. & Bretherton, C. S. On the relationship between stratiform low cloud cover and lower-tropospheric stability. *Journal of Climate* **19**, 6425–6432 (2006).

[29] Saxena, A. *et al.* A review of clustering techniques and developments. *Neurocomputing* **267**, 664–681 (2017). URL https://www.sciencedirect.com/science/article/pii/S0925231217311815.

[30] Bock, H.-H. *Clustering Methods: A History of k-Means Algorithms*, 161–172 (Springer Berlin Heidelberg, Berlin, Heidelberg, 2007). URL https://doi.org/10.1007/978-3-540-73560-1_15.

[31] Jia, H., Quaas, J., Gryspeerdt, E., Böhm, C. & Sourdeval, O. Addressing the difficulties in quantifying droplet number response to aerosol from satellite observations. *Atmospheric Chemistry and Physics* **22**, 7353–7372 (2022).

[32] Schmidt, J., Ansmann, A., BÃŒhl, J. & Wandinger, U. Strong aerosol-cloud interaction in altocumulus during updraft periods: Lidar observations over central europe. *Atmospheric Chemistry and Physics* **15**, 10687–10700 (2015).

[33] Quaas, J. *et al.* Constraining the Twomey effect from satellite observations: Issues and perspectives. *Atmospheric Chemistry and Physics* **20**, 15079–15099 (2020).

[34] Gryspeerdt, E., Stier, P., White, B. A. & Kipling, Z. Wet scavenging limits the detection of aerosol effects on precipitation. *Atmospheric Chemistry and Physics* **15**, 7557–7570 (2015).

[35] McComiskey, A. & Feingold, G. The scale problem in quantifying aerosol indirect effects. *Atmospheric Chemistry and Physics* **12**, 1031–1049 (2012).

[36] Sinclair, K. *et al.* Inference of precipitation in warm stratiform clouds using remotely sensed observations of the cloud top droplet size distribution. *Geophysical Research Letters* **48**, e2021GL092547 (2021). URL https://agupubs.onlinelibrary.wiley.com/doi/abs/10.1029/2021GL092547. E2021GL092547 2021GL092547, https://agupubs.onlinelibrary.wiley.com/doi/pdf/10.1029/2021GL092547.

[37] Dzambo, A. M. *et al.* Joint cloud water path and rainwater path retrievals from airborne oracles observations. *Atmospheric Chemistry and Physics* **21**, 5513–5532 (2021).